Modal interaction matrix measurement for liquid-crystal corrector: precision evaluation

Quanquan Mu,[1, 2] Zhaoliang Cao,[1,*] Zenghui Peng,[1] Yonggang Liu,[1] Lifa Hu,[1] Xinghai Lu,[1] and Li Xuan[1]

[1]*State Key Lab of Applied Optics, Changchun Institute of Optics, Fine Mechanics and Physics, Chinese Academy of Sciences, Changchun, Jilin 130033, China*
[2]*Graduate School of the Chinese Academy of Sciences, Beijing 100039, China*
caozlok@yahoo.com.cn

Abstract: A modal interaction matrix (IM) measurement procedure is introduced for a liquid-crystal (LC) corrector for use in a phase-wrapping technique. Zernike modes are used to reconstruct the aberration wavefront and to drive the LC corrector. Usually the driving area is different from the active area. This difference induces a coupling effect on Zernike modes, which may have an impact on correction precision. In this paper the coupling effect is evaluated due to area difference and decentration, respectively. Then, a simulated turbulence wavefront is used to simulate the reconstruction process to evaluate its influence on reconstruction precision. We present simulation results that show that this method can be used to measure the IM with very high reconstruction precision under proper configuration. In order to maintain precision, the permissible eccentricity distance is also simulated with a result of no more than 5% of the LC corrector diameter.

OCIS codes: (010.1080) Active or adaptive optics; (230.3720) Liquid-crystal devices.

References and links

1. Z. Hu and W. Jiang, "Optimum the matching problem of wavefront sensor and wavefront corrector," *High Power Laser and Particle Beams* (in Chinese) **8**, 327–332 (1996).
2. S. R. Restaino, D. M. Payne, J. T. Baker, J. R. Andrews, S. W. Teare, G. C. Gilbreath, D. Dayton, and J. Gonglewski, "Liquid-crystal technology for adaptive optics: an update," SPIE **5003**, 187–192 (2003).
3. L. Hu, L. Xuan, Y. Liu, Z. Cao, D. Li, and Q. Mu, "Phase-only liquid-crystal spatial light modulator for wavefront correction with high precision," Opt. Express **12**, 6403–6409 (2004).
4. Q. Mu, Z. Cao, L. Hu, D. Li, and L. Xuan, "Adaptive-optics imaging system based on a high-resolution liquid crystal on silicon device," Opt. Express **14**, 8013–8018 (2006).
5. K. A. Bauchert, S. A. Serati, and A. Furman, "Advances in liquid-crystal spatial light modulators," SPIE **4734**, 35–43 (2002).
6. H. Huang, T. Inoue, and T. Hara, "An adaptive wavefront control system using a high-resolution liquid-crystal spatial light modulator," SPIE **5639**, 129–137 (2004).
7. Q. Mu, Z. Cao, C. Li, B. Jiang, L. Hu, and L. Xuan, "Accommodation-based liquid-crystal adaptive optics system for large ocular aberration correction," Opt. Lett. **33**, 2898–2900 (2008).
8. G. D. Love, "Wavefront correction and production of Zernike modes with a liquid-crystal spatial light modulator," Appl. Opt. **36**, 1517–1520 (1997).
9. L. Thibos, R. A. Applegate, J. T. Schwiegerling, and R. Webb, "Standards for reporting the optical aberrations of eyes," in Vision Science and its Applications, OSA Technical Digest (Optical Society of America, 2000), paper SuC1.
10. J. Schwiegerling, "Scaling Zernike expansion coefficients to different pupil sizes," J. Opt. Soc. Am. A **19**, 1937–1945 (2002).
11. L. Lundström and P. Unsbo, "Transformation of Zernike coefficients: scaled, translated, and rotated wavefronts with circular and elliptical pupils," J. Opt. Soc. Am. A **24**, 569–577 (2007).

#109113 - $15.00 USD Received 23 Mar 2009; revised 17 Apr 2009; accepted 28 Apr 2009; published 19 May 2009

1. Introduction

Adaptive optics is used to enhance the capability of optical systems by actively compensating for aberrations. A commonly used adaptive optics system consists of three subsystems. A wavefront sensor (WFS) [usually a Hartmann–Shack (H–S) WFS] measures the distortions. A wavefront corrector (WFC) usually using a continuous facesheet deformable mirror (DM) can rapidly change its surface shape to compensate for distortions measured by a WFS. A control computer is used to receive the WFS measurement and translate it into control signals to drive the WFC. The translation procedure is accomplished by the interaction matrix (IM), which relates the DM actuator commands to the WFS measurement. So, the precision of the IM will influence correction precision.

For a conventional continuous facesheet DM, the arrangement of actuators on the WFC and the lenslet array on the H–S sensor should be in proper configuration [1]. Then, the static response of each actuator is measured individually. These responses give the columns of the IM.

A liquid-crystal (LC) corrector is an alternative selection for adaptive optics due to its low cost, reliability, low power consumption, low price, lack of moving mechanical components, and high resolution [2–6]. It has millions of pixels, which makes it possible to use the phase-wrapping technique to increase its modulation depth without any loss of spatial resolution [7]. Due to the use of this technology, it is impossible to drive each single pixel to get the IM. In this paper, a Zernike polynomial-based modal IM calculation procedure is introduced. A set of Zernike polynomials is used to reconstruct the aberration wavefront and drive the LC corrector. The driving area of the LC corrector is usually larger than the active area for compensation in order to eliminate edge alignment error. The scale factor (SF), which is defined as the ratio of the radius of the active area and the driving area, is used to represent this area difference. This difference will induce a coupling effect on Zernike modes, which may impact correction precision. Here, we evaluated the coupling effect due to the area difference and decentration, respectively. Then, a simulated turbulence wavefront is used to simulate the reconstruction process to evaluate its influence on reconstruction precision. We assume the LC corrector is square with K×K pixels. The IM and the reconstruction error are calculated for different SF and K. The relationship between the reconstruction error with SF, K, and decentration is discussed.

2. Calculation of the IM

As we know, the pixel response of an LC corrector is piston-like, with the modulation depth nearly one wavelength in the visible range [8]. In order to increase its modulation depth, the phase-wrapping technique was used. In this condition, the control method used for the DM is no longer suitable for an LC corrector. We introduced a Zernike polynomial-based modal method to accomplish this. The Zernike polynomials are a set of functions that are orthogonal over the unit circle. This is defined as

$$Z_i(r,\theta) = \begin{cases} N_n^m R_n^{|m|}(r)\cos(m\theta), & m \geq 0 \\ -N_n^m R_n^{|m|}(r)\sin(m\theta), & m < 0 \end{cases},$$

where

$$R_n^{|m|}(r) = \sum_{s=o}^{(n-|m|)/2} \frac{(-1)^s (n-s)!}{s![(n+|m|)/2-s]![(n-|m|)/2-s]!} r^{n-2s},$$

where $0 \leq r \leq 1$, N_n^m is the normalization factor, and $0 \leq \theta \leq 2\pi$; n is a non-negative integer and m varies from $-n$ to n with a step of 2 [9].

The configuration of the LC corrector is shown in Fig. 1. The solid circle with radius r_2 represents the driven area, which is the inscribed circle of the LC corrector. Only the area in

#109113 - $15.00 USD Received 23 Mar 2009; revised 17 Apr 2009; accepted 28 Apr 2009; published 19 May 2009

the dashed circle with radius r_1 is active for detection, which is actually matched with the telescope pupil used for compensation. The SF is equal to r_1 / r_2. This configuration can eliminate accurate pupil alignment, which improves the system ease of fabrication. Otherwise, any missed alignment at the pupil edge will induce a correction error.

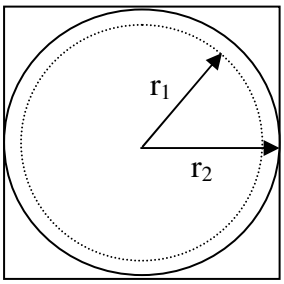

Fig. 1. Configuration of LC corrector.

Because $r_1 < r_2$, the wavefront detected in r_1 is the part of the LC corrector generated in r_2. For instance, we generated only the ith Zernike mode on the LC corrector. The H–S sensor detected in r_1 is a serial of Zernike polynomials. This can be expressed as

$$Z_i(r_2,\theta_2) = \sum_{j=1}^{N} M_{i,j} Z_j(r_1,\theta_1) \text{ , when } 0 \le r_2 \le r_1; 0 \le r_1 \le 1,$$

where $M_{i,j}$ is the jth Zernike coefficient detected for ith Zernike polynomial.

Here, we used the phase values in r_1 to directly reconstruct the detection wavefront into Zernike polynomials to simulate the H–S sensor detection process. Under this procedure, the *IM M*[*N, N*] for all the *N* Zernike polynomials was measured.

For an aberration that has a series of coefficients $a_j (1 \le j \le N)$, the reconstruction coefficients $c_i (1 \le i \le N)$ can be calculated by

$$\begin{bmatrix} c_1 \\ \vdots \\ c_i \\ \vdots \\ c_N \end{bmatrix} = \begin{bmatrix} M_{1,1} & \cdots & M_{1,j} & \cdots & M_{1,N} \\ \vdots & \ddots & & & \vdots \\ M_{i,1} & & M_{i,j} & & M_{i,N} \\ \vdots & & & \ddots & \vdots \\ M_{N,1} & \cdots & M_{N,j} & \cdots & M_{N,N} \end{bmatrix}^{-1} \begin{bmatrix} a_1 \\ \vdots \\ a_j \\ \vdots \\ a_N \end{bmatrix}$$

3. The distribution of IM

First, we assumed that the two circles were concentric to simulate the IM measurement procedure just to evaluate the influence of SF. For each Zernike mode we sent to the LC corrector, the detected coefficients were reconstructed by the phase values in circle r_1. The columns of the IM were calculated for the LC corrector when K=400 and SF=0.86, as shown in Fig. 2. The Zernike modes 1, 2, 3, 4, 5, 6, 9, 10, 14, 15, 20, 21, 27, 28, and 35 remained orthogonal with lower amplitude, as shown in Fig. 2(a). All other modes revealed the coupling effect, as shown in Figs. 2(b)–2(e). Due to the coupling effect, the maximum amplitude appeared at the proximate coupling mode, not at the mode itself. From this profile we conclude that all the modes coupled to those corresponding modes, which have the same

#109113 - $15.00 USD Received 23 Mar 2009; revised 17 Apr 2009; accepted 28 Apr 2009; published 19 May 2009

azimuthal frequency but lower radial frequency if they exist, are shown in Fig. 3. It indicates that Zernike modes located at both side of the triangle have no coupling element. The coupling effect is represented by the red arrow lines. The coupling effect and the amplitude of each Zernike mode are compared with the calculation taken by Schwiegerling [10]. They match very well, which proves that this simulation procedure is valid.

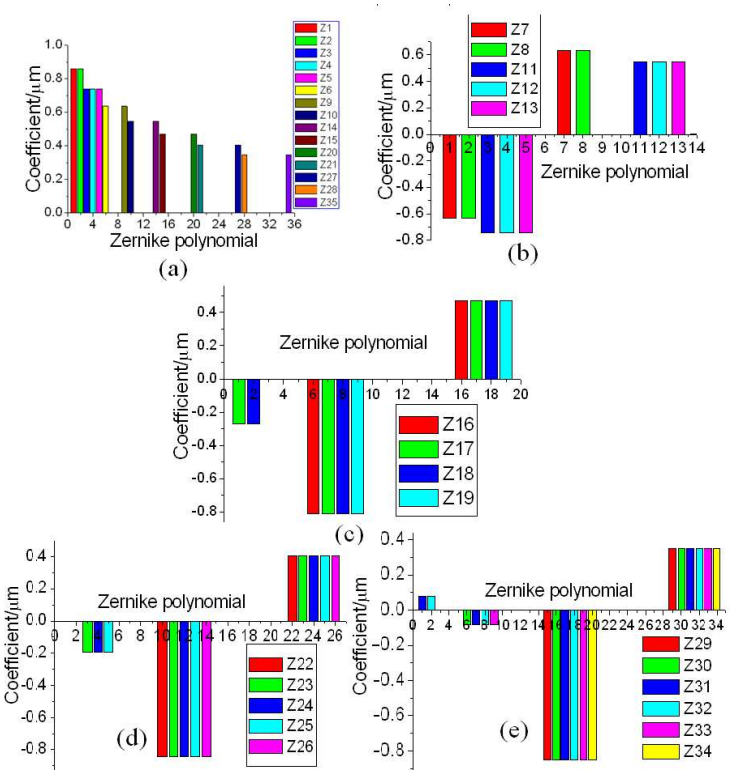

Fig. 2. IM coefficient profile.

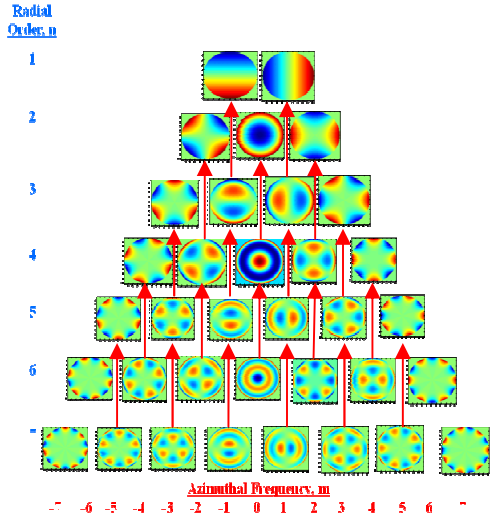

Fig. 3. Coupling relationship of all 35 polynomials.

#109113 - $15.00 USD Received 23 Mar 2009; revised 17 Apr 2009; accepted 28 Apr 2009; published 19 May 2009

After this, the decentration was considered. This situation may appear due to central misalignment. According to our calculation, we found that all the Zernike modes shown had coupling effects and became more complicated. Figure 4 illustrates the distribution of IM when K=400 and SF=0.8. The eccentricity distance was 40 pixels along the 45° direction. For different eccentricity distances and directions, they had different distributions and amplitudes. This phenomenon was also proved by Lundström [11].

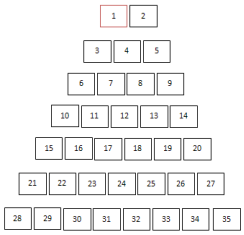

Fig. 4. Distribution of IM at decentration condition (Media 1).

4. Evaluation of the reconstruction precision

The previous discussion indicates that the coupling effect was influenced by the SF and decentration. This influence may induce reconstruction errors when used for wavefront correction. In this section, we discuss this reconstruction precision for different SFs, Ks, and decentration.

4.1 The influence of SF and K

At first, we assumed that the two circles on the LC corrector were concentric. A simulated turbulence wavefront represented by the Zernike polynomial, shown in Fig. 5, was used to evaluate this influence. The peak-to-valley (PV) and root mean square (rms) values were 2.2264 μm and 0.854 μm, respectively. The reconstruction error map was expressed as

$$\text{error}(r_1,\theta_1)=\sum_{i=1}^{N}c_iZ_i(r_2,\theta_2)-\sum_{j=1}^{N}a_jZ_j(r_1,\theta_1)\quad \text{when } 0\le r_2\le r_1;0\le r_1\le 1,$$

where $\sum_{j=1}^{N}a_jZ_j(r_1,\theta_1)$ and $\sum_{i=1}^{N}c_iZ_i(r_1,\theta_2)$ represent the simulated and reconstructed wavefronts, respectively.

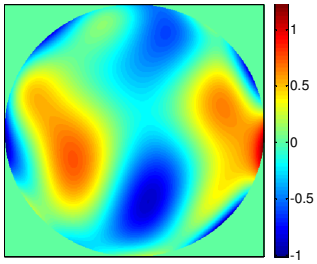

Fig. 5 The simulated turbulence map.

For an LC corrector that has K×K pixels, the rms value of the reconstruction error can be calculated by all the $(K\times SF)^2$ discrete values of the error map. The dots in Fig. 6 illustrate the rms values of the reconstruction error with different SFs for K=100, 200, 256, and 400. For a given LC corrector, it decreases when the SF increases. This value will trend to zero when SF=1, no matter how many pixels the corrector has.

#109113 - $15.00 USD Received 23 Mar 2009; revised 17 Apr 2009; accepted 28 Apr 2009; published 19 May 2009

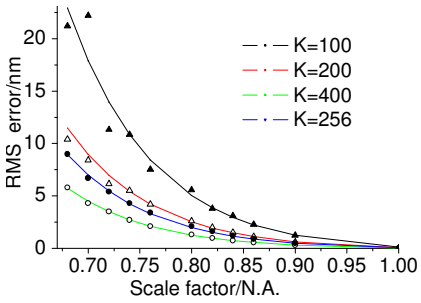

Fig. 6. Rms error for different SF and K.

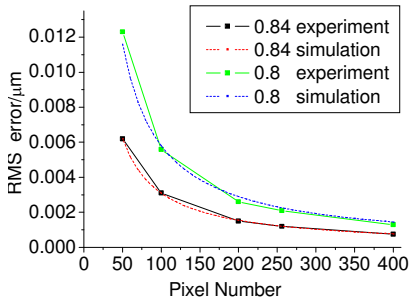

Fig. 7. Relationship between rms error and K.

For a fixed SF, the rms error also changes with K. Figure 7 illustrates this change when SF=0.84 and 0.8. They obey the $y = a / x$ law with coefficients $a = 0.31$ and $a = 0.58$, respectively. Under this relationship, we educed the formula between the rms error, SF, and K with exponential fit, as shown below:

$$RMS(K, SF) = K^{-1} \times \left(-0.0356 + 9302 \times e^{(-SF/0.082)} \right).$$

The solid curve in Fig. 6 shows the fitted value. They match with the dots very well.

4.2 The influence of decentration

At the decentration condition, the reconstruction error will be different for different eccentricity distances and directions. Figure 8 illustrates the rms error with different eccentricity distances along the vertical direction when K=400, SF=0.8, and 0.75. The eccentricity distance is represented by the pixel number between the centers of the two circles. This indicates that the rms error does not increase when the distance is smaller than 20, which is 5% of K. This percentage is also supported by other K and SF configurations. This means that for a fixed pupil diameter, no matter how many pixels we use, the maximum permissible decentration is 5% of the diameter.

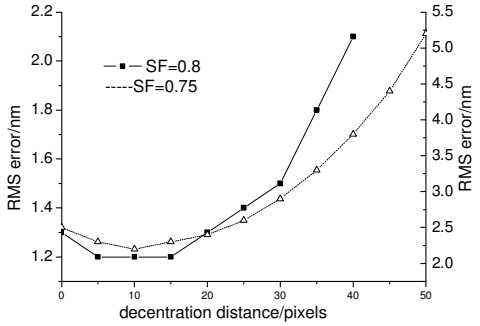

Fig. 8. Rms error induced by decentration.

5. Discussions and conclusions

In this paper, a Zernike polynomial-based modal method was introduced to simulate the IM measurement and wavefront reconstruction process for an LC corrector by the use of the phase-wrapping technique. The driving area of the LC corrector was always its inscribed circle for simple control. The active area, which was conjugated with the telescope pupil, was smaller than the driving area. The SF was used to represent this area difference. The mode

#109113 - $15.00 USD Received 23 Mar 2009; revised 17 Apr 2009; accepted 28 Apr 2009; published 19 May 2009

coupling effect induced by the SF was discussed. We concluded that at concentric conditions, all the modes coupled to those corresponding modes that have the same azimuthal frequency but a lower radial frequency, if they exist. The influence on the reconstruction precision was discussed with a simulated turbulence wavefront map for different SFs and Ks. We educed the formula between the rms error, SF, and K with exponential fit. This expression was just for the example wavefront used in the simulation. In the near future we will attempt to find the exact relationship considering the influence of the original aberration. For a different turbulence, we should choose an appropriate LC corrector and SF to attain an acceptable correction precision. At the decentration condition, the coupling effect becomes more complicated. In order to maintain the reconstruction precision, the eccentricity distance should restrict no more than 5% of the LC corrector diameter.

Acknowledgments

This work is supported by the National Natural Science Foundation of China grants 60736042, 60578035 and 50703039.

#109113 - $15.00 USD Received 23 Mar 2009; revised 17 Apr 2009; accepted 28 Apr 2009; published 19 May 2009